

# High explosive thermodynamic equations of state for combined fragmentation and blast loading

E. L. Baker<sup>1</sup>, G. M. Stunzenas, L. I. Stiel<sup>2</sup>, D. Murphy<sup>1</sup> & A. Enea<sup>1</sup>

<sup>1</sup>*US Army Armament Research Development and Engineering Center, USA*

<sup>2</sup>*New York Polytechnic University, USA*

## Abstract

There is an increasing emphasis on the modeling of security related blast events that produce both fragmentation and blast loading. The Jones-Wilkins-Lee-Baker (JWL) thermodynamic equation of state was originally developed to more accurately describe overdriven detonation, while maintaining an accurate description of high explosive products early expansion work output associated with metal pushing and fragmentation. The equation of state is more mathematically complex than the Jones-Wilkins-Lee equation of state, as it includes an increased number of parameters to describe the principle isentrope, as well as a Gruneisen parameter formulation that is a function of specific volume. Although the increased mathematical complexity over JWL was originally implemented in order to model both overdriven detonation and early volume expansion work output, it has been found that this increased mathematical complexity also allows the flexibility to parameterize higher volume work output associated with blast output. As increased numbers of parameters can mean increased calibration complexity and does not guarantee increased accuracy for practical problems of interest, calibration techniques have been developed to provide robust detonation products equation of state parameters that are applicable to the broad range of high explosive work output associated with overdriven detonation (wave shapers), early volume expansion (metal pushing) and late volume expansion (blast). This paper presents a method of parameter calibration: formal optimization using JAGUAR thermo-chemical predictions to cylinder test and high volume total work output associated with blast overpressure and impulse. The calibration procedure details are presented,



along with equation of state parameter sets and ALE3D modeling comparisons. Although reasonable agreement to empirically based peak overpressures is achieved, the results indicate that an explosive products afterburning model is required to achieve further agreement with empirically based peak overpressures and impulse.

*Keywords: blast, explosives, equation of state, shock, impulse, modelling.*

## 1 Introduction

There is an increasing emphasis on the modelling of security related blast events that produce both fragmentation and blast loading. The combined loading of blast and fragments, caused by explosions, is known to often produce damage greater than the sum of the damage caused by the blast and fragment loading treated separately. This phenomenon is well known and is pointed out in literature and design manuals within the area of protective design [1]. However, due to a lack of more sophisticated modelling [2] and the complex nature of combined blast and fragment loading, the design manuals normally disregard the effect or treat it in a very simplified manner [1]. One missing aspect for combined blast and fragment loading modelling, is the development of detonation products equations of state that are accurate for a broad range of volume expansions. This is required in order to predict the fragmentation characteristics produced at early detonation products volume expansion, as well as to predict the total work output produced at very high detonation products volume expansions. The Jones-Wilkins-Lee-Baker (JWL) thermodynamic equation of state was investigated in an effort to accurately predict both early volume expansion and highly expanded behaviour associated with air blast. In this study, the explosives TNT and LX-14 were used for computational investigations.

## 2 Jones-Wilkins-Lee-Baker equation of state

The Jones-Wilkins-Lee-Baker (JWL) thermodynamic equation of state was originally developed to more accurately describe overdriven detonation, while maintaining an accurate description of high explosive products early expansion work output associated with metal pushing and fragmentation [3]. The equation of state is more mathematically complex than the Jones-Wilkins-Lee equation of state, as it includes an increased number of parameters to describe the principle isentrope, as well as a Gruneisen parameter formulation that is a function of specific volume. The JWL mathematical form is:

$$P = \sum_n A_i \left( 1 - \frac{\omega}{R_i V^*} \right) e^{-R_i V^*} + \frac{\lambda E}{V^*} \quad (1)$$

$$\lambda = \sum_i (A_{\lambda i} V^* + B_{\lambda i}) e^{-R_{\lambda i} V^*} + \omega \quad (2)$$



where  $V^*$  is the relative volume,  $E$  is the product of the initial density and specific internal energy and  $\lambda$  is the Gruneisen parameter. Although the increased mathematical complexity over the Jones-Wilkins-Less (JWL) equation of state was originally implemented in order to model both overdriven detonation and early volume expansion work output, it has been found that this increased mathematical complexity also allows the flexibility to parameterize higher volume work output associated with blast output. As increased numbers of parameters can mean increased calibration complexity and does not guarantee increased accuracy for practical problems of interest, calibration techniques have been developed to provide robust detonation products equation of state parameters that are applicable to the broad range of high explosive work output associated with early volume expansion (metal pushing) and late volume expansion (blast).

### 3 JWL equation of state calibration

For this study, the JWL equation of state was parameterized for early volume expansion through the use of JAGUAR thermo-chemical equation of state calculations for detonation properties and associated cylinder test velocities. Formal optimization was used to parameterize JWL for TNT and LX-14. The early volume detonation state and early volume expansion cylinder velocities were held constant, while the high volume work output associated with isentropic expansion was adjusted to increasingly higher values in order to approximate the energy output associated with explosive products afterburning.

#### 3.1 Detonation and cylinder velocity calculations

JAGUAR analytical procedures have been developed for the accurate calculation of detonation properties and cylinder test products expansion for H-C-N-O near ideal explosives. These routines use extended JCZ3 thermo-chemical equation of state procedures with EXP-6 potentials for H-C-N-O detonation products [4]. An analytic cylinder test model has long been used by ARDEC for explosive equation of state calibration and verification [5]. This analytic model has been shown to provide close agreement to high rate continuum modelling. The analytic model is based on adiabatic expansion along the principle isentrope from the Chapman-Jouguet state. Figure 1 presents a sketch of the analytic cylinder test model and ALE3D modelling of a cylinder test.

ALE3D high rate continuum modelling was compared to analytic cylinder test modelling using identical JWL equations of state for TNT and LX-14. The JWL equations of state were parameterized using JAGUAR thermo-chemical equation of state modelling [5]. Two different copper cylinder thicknesses, 1.2" OD, 1" ID 10" long and 1.3" OD, 1" ID 10" long, was modelled using the Johnson-Cook material model. Figure 2 presents the comparison of the analytic cylinder test model to the ALE3D modelling for TNT and LX-14 respectively.



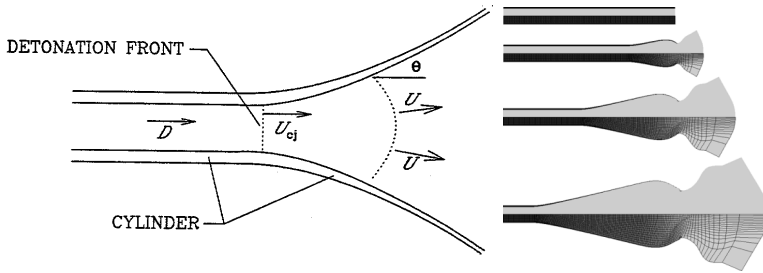


Figure 1: Analytic cylinder model (left) and ALE3D cylinder modelling (right).

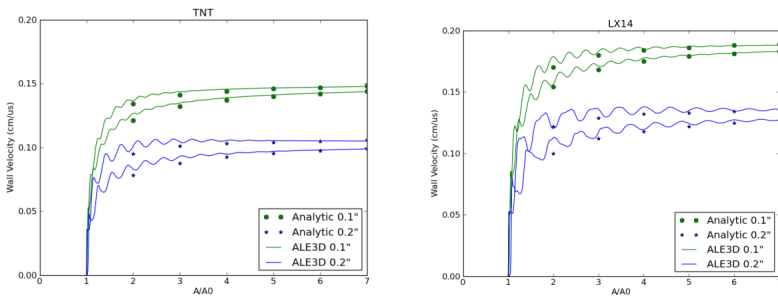


Figure 2: TNT (left) and LX-14 (right) analytic cylinder model results compared to ALE3D calculations.

For each pair of curves, the higher curve represents the velocity history of the inside of the copper cylinder and the lower curve represents the velocity history of the outside of the cylinder. The analytic cylinder model slightly under predicts the velocities at 2 and 3 inside area expansions, but is in very close agreement by 6 and 7 inside area expansions. This is consistent with the fact that this analytic modeling approach neglects initial acceleration due to shock processes. Strong shock effects are typically observed in the 2 to 3 volume expansion region and are significantly damped out by 6 volume expansions, where very close agreement between the analytic model and ALE3D results are observed.

### 3.2 High volume products expansion and blast calibration

For the modified total work output JWL equations of state, the detonation state and early volume expansion cylinder velocities were held constant, while the high volume work output associated with isentropic expansion to ambient pressure was adjusted to increasingly higher values. This increased total work output was incorporated in order to approximate the energy output associated with explosive products afterburning, as both TNT and LX-14 are negatively oxygen balanced (TNT: -74%, LX-14: -29.5%). Table 1 presents the standard TNT JWL parameters. Table 2 presents the TNT and LX-14 JWL parameters

Table 1: Standard JWL parameter sets.

<b>Explosive</b>	TNT	LX-14
<b>E0 (Mbar)</b>	0.0662	0.101
<b>Density (g/cc)</b>	1.59	1.835
<b>Mass (g)</b>	2212.3101	2553.20065
<b>Gamma+1</b>	4.0919194	3.75486
<b>A (Mbar)</b>	7.967686	7.558595
<b>B (Mbar)</b>	0.146069	0.2268433
<b>R1</b>	5.5	4.44
<b>R2</b>	1.3	1.5
<b>W</b>	0.3	0.3
<b>D (cm/microsecond)</b>	0.698	0.883

Table 2: Increased total work output JWLb parameter sets.

<b>Explosive</b>	TNT	TNT	TNT	LX-14	LX-14	LX-14
<b>E0 (Mbar)</b>	0.075	0.085	0.095	0.1025	0.1035	0.135
<b>Dens (g/cc)</b>	1.63	1.63	1.63	1.82	1.82	1.82
<b>Mass (g)</b>	2267.96	2267.96	2267.96	2532.33	2532.33	2532.33
<b>Gamma+1</b>	3.91913	3.91913	3.91913	3.04639	3.04653	3.04653
<b>A1</b>	4.9333E+02	5.0001E+02	5.0000E+02	5.0001E+02	3.9919E+02	4.9969E+02
<b>A2</b>	1.3770E+02	9.6084E+00	9.3619E+00	9.7672E+00	5.0086E+01	9.4381E+00
<b>A3</b>	1.1138E+00	1.7877E+00	3.2315E+00	3.5460E+00	1.4099E+00	6.7552E+00
<b>A4</b>	1.1333E-02	-9.7788E-22	2.0880E+00	3.4401E-28	4.9131E-03	1.1444E-22
<b>R1</b>	3.5248E+01	1.4020E+01	1.5805E+01	1.3020E+01	2.8562E+01	1.5109E+01
<b>R2</b>	1.1381E+01	1.3990E+01	1.5572E+01	1.2989E+01	8.3481E+00	1.5203E+01
<b>R3</b>	2.7172E+00	3.2798E+00	4.0420E+00	3.4490E+00	2.4622E+00	4.2517E+00
<b>R4</b>	2.7403E-01	3.3133E-01	3.8038E-01	4.0269E-01	4.2812E-01	1.0119E+00
<b>C0 (Mbar)</b>	1.0982E-02	1.5845E-02	2.0708E-02	2.8961E-02	1.1795E-02	3.6793E-02
<b>W</b>	2.8108E-01	2.8108E-01	2.8108E-01	3.6677E-01	3.6677E+00	3.6677E-01
<b>AL1</b>	6.1607E+00	6.1607E+00	6.1607E+00	4.7155E+01	4.7155E+01	4.7155E+01
<b>AL2</b>	2.0283E+01	2.0283E+01	2.0283E+01	5.2212E+00	5.2212E+00	5.2212E+00
<b>BL1</b>	-2.8103	-2.8103	-2.8103	3.2210	3.2210	3.2210
<b>BL2</b>	7.4495	7.4495	7.4495	-3.2648	-3.2648	-3.2648
<b>RL1</b>	1.76848	1.76848	1.76848	27.3809	27.3809	27.3809
<b>RL2</b>	26.2612	26.2612	26.2612	1.49825	1.49825	1.49825
<b>D (cm/<math>\mu</math>s)</b>	6.8179E-01	6.8179E-01	6.8179E-01	8.6324E-01	8.6324E-01	8.6324E-01



for the modified total work output study. Table 3 presents the analytically predicted cylinder velocities and associated predicted Gurney constants associated with each of the modified total work output JWL parameter sets using a 1" ID and 1.2" OD copper cylinder. The presented cylinder velocities and Gurney energies demonstrate that although the modified work output JWL parameter sets have increased total work output  $E_0$  values, the equation of states maintain the same predicted cylinder velocities and associated early volume expansion characteristics.

Table 3: Modified total work output JWL predicted cylinder velocities for a 1" ID, 1.2" OD copper tube.

Explosive	$E_0$ (Mbar)	Cylinder Volume Expansion (A/A0)	Analytic Inside Cylinder Velocity (cm/ $\mu$ s)	Analytic Outside Cylinder Velocity (cm/ $\mu$ s)	Gurney constant (cm/ $\mu$ s)
TNT	0.075	2	0.130889091	0.137144785	0.202167448
		5	0.143051938	0.137144785	0.233973672
		7	0.145943951	0.141562639	0.241510681
TNT	0.085	2	0.125542523	0.113660859	0.193909295
		5	0.141877562	0.136018903	0.232052879
		7	0.146201877	0.141812823	0.241937503
TNT	0.095	2	0.119447602	0.108142778	0.18449526
		5	0.140724121	0.134913092	0.230166328
		7	0.146427035	0.142031221	0.242310098
LX-14	0.1025	2	0.160033448	0.144887476	0.236255505
		5	0.180708841	0.173246693	0.282498434
		7	0.185932388	0.180350604	0.294082168
LX-14	0.1035	2	0.170929044	0.154751885	0.252340547
		5	0.184720626	0.177092816	0.288769975
		7	0.186802397	0.181194494	0.295458227
LX-14	0.135	2	0.152699824	0.138247925	0.225428962
		5	0.178989614	0.171598459	0.279810801
		7	0.1856975	0.180122766	0.293710654

### 3.3 Blast calculations

ALE3D was used to model the explosive detonation and subsequent blast produced by using standard JWL equations of state and modified total work output JWL equations of state. Air was modelled using the ideal gas equation of state with an adiabatic gamma of 1.4. A 13.85 cm diameter sphere of high explosive was detonated in the centre of a high resolution mesh consisting of 5

million cells on a 200 cm cube. Tracer particles were placed at 9 positions evenly spaced from 2.5 foot (76.2 cm) to 6.5 foot (198.1 cm) from the charge center. Figure 3 presents pressure colour plots from the computations at 30, 200 and 500 microseconds.

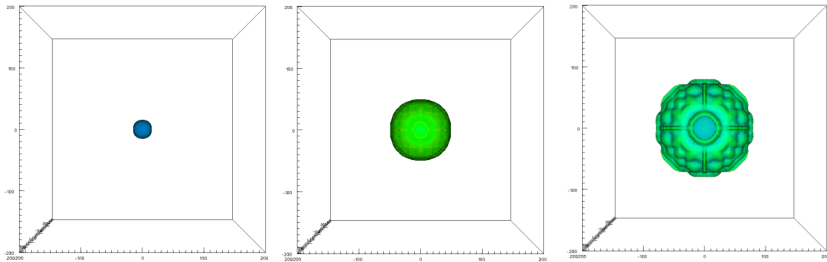


Figure 3: TNT air blast computation pressure plots at 30, 200 and 500 $\mu$ s.

Figure 4 presents the TNT peak overpressure computational results as a function of distance. Figure 5 presents the TNT incident impulse air blast computational results as a function of distance. Figure 6 presents the LX-14 peak overpressure computational results as a function of distance. Figure 7 presents the LX-14 incident impulse air blast computational results as a function of distance. The results are compared to empirically based analytic calculations from CONWEP [6].

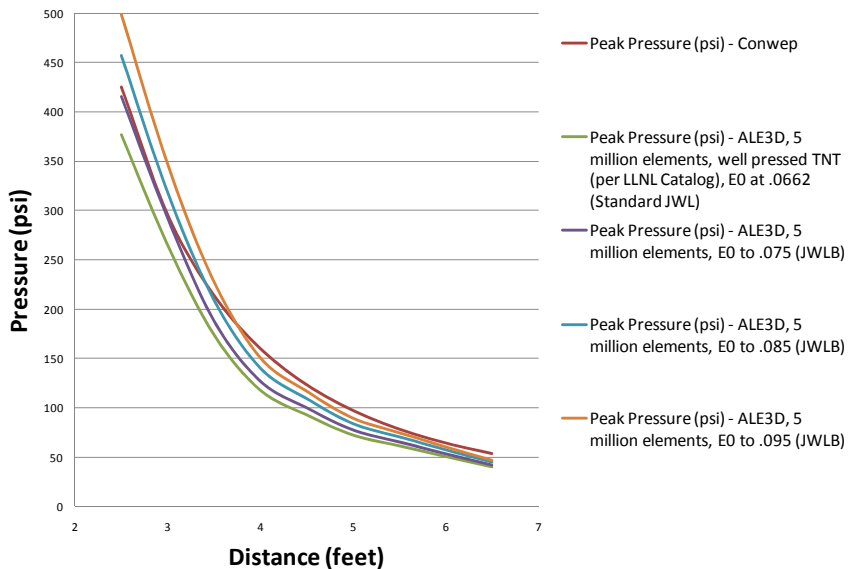


Figure 4: TNT peak overpressure computational results as a function of distance.

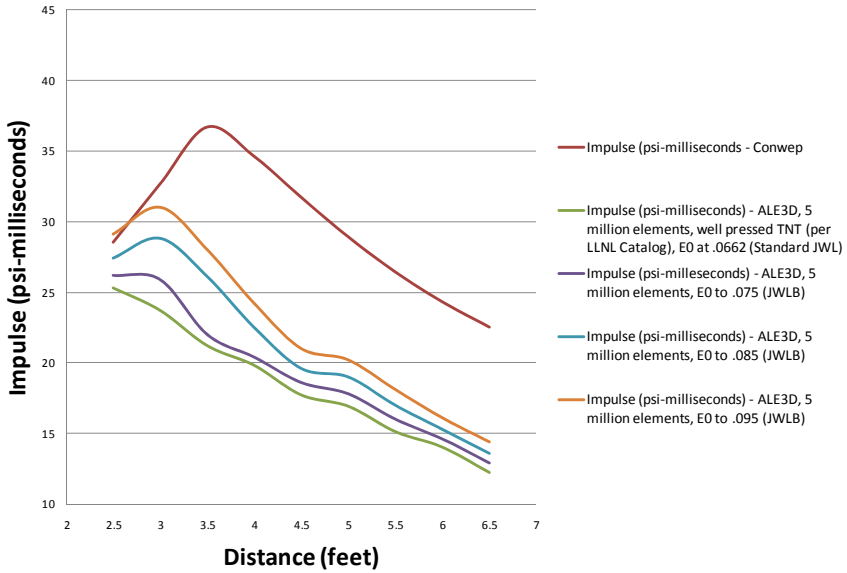


Figure 5: TNT blast incident impulse results as a function of distance.

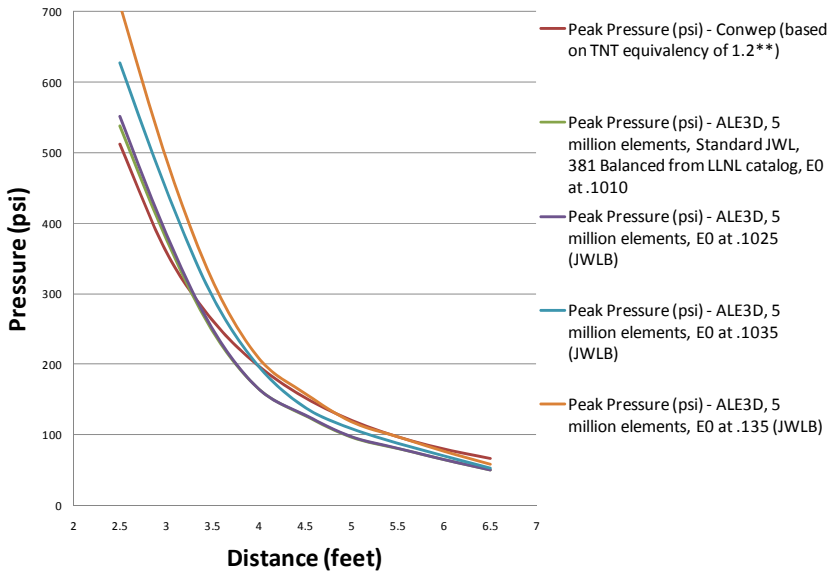


Figure 6: LX-14 peak overpressure results as a function of distance.



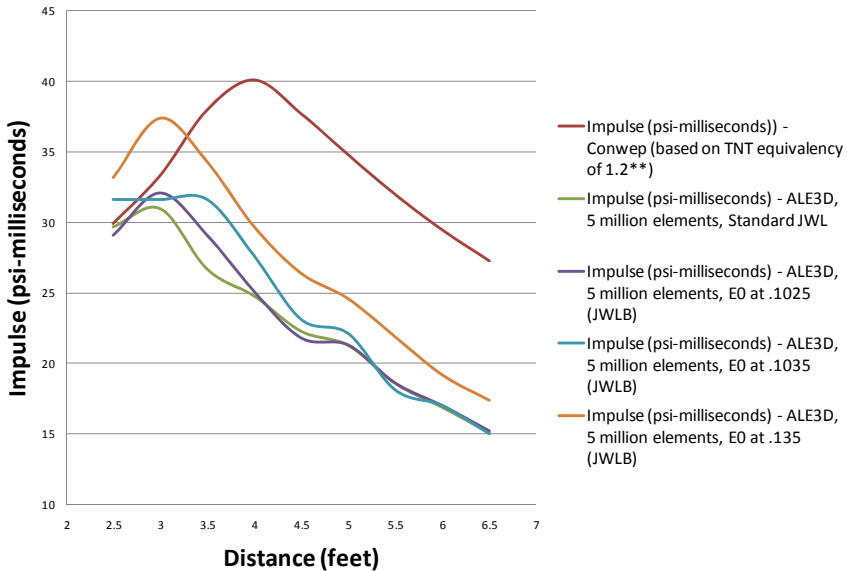


Figure 7: LX-14 blast incident impulse results as a function of distance.

## 4 Conclusions

It is possible to produce increased total work output using the JWL equation of state, while maintaining agreement accepted detonation characteristics and cylinder test data. This was done in an attempt to account for explosive detonation products afterburning with air, while avoiding the use of potentially inaccurate and computationally expensive air mixing, diffusion and combustion models. This modified equation of state approach seems reasonable, as it can be viewed as an analogous approach to the currently used empirical blast scaling. It is clear from the computational results, that agreement with empirical peak blast overpressures can be achieved and that the trend moving towards agreement incident blast impulse occurs as the total work output is increased. However, reasonable parameter sets become increasingly difficult to achieve as the total work output is increased. This is due to the difficulty in maintaining agreement with cylinder velocity values consistent with early detonation products expansion up to 7 times the initial unreacted explosive volume. Although reasonable agreement to the empirically based peak overpressures can be achieved, the results indicate that an explosive products afterburning model is required to achieve further agreement with empirically based peak overpressures and impulse. There is clear evidence of the effect of afterburning [7] with limited practical high rate continuum model development [8, 9] to date. One potential simplified approach is to use a partial equilibrium equation of state that was previously used successfully for the modeling of combined effects explosives aluminum reaction [10].

## References

- [1] E.J. Conrath, Structural design for physical security– state of the practice. American Society of Civil Engineers Task committee, Reston, VA, USA, 1999 (p. 264).
- [2] U. Nyström and K. Gylltoft, Numerical studies of the combined effects of blast and fragment loading, *International Journal of Impact Engineering*, Volume 36, Issue 8, August 2009, (p. 995-1005).
- [3] E.L. Baker, An application of variable metric nonlinear optimization to the parameterization of an extended thermodynamic equation of state”, *Proceedings of the Tenth International Detonation Symposium*, Edited by J. M. Short and D. G. Tasker, Boston, MA, pp. 394-400, July 1993.
- [4] L.I. Stiel, and E.L. Baker, Detonation energies of explosives by optimized JCZ3 procedures, *Proceedings of the APS Topical Conference on Shock Compression of Condensed Matter*, New Hampton, MA, August 1997.
- [5] E.L. Baker, and L.I. Stiel, Improved cylinder test agreement with JAGUAR optimized extended JCZ3 procedures”, *Proceedings of the International Workshop on New Models and Numerical Codes for Shock Wave Processes in Condensed Media*, St. Catherines College, Oxford, UK, September 1997.
- [6] D.W. Hyde, Microcomputer programs CONWEP and FUNPRO, applications of TM 5-855-1, Instructions Report SL-88-1 (ADA195867), Structure Lab, Army Engineer Waterways Experiment Station, Vicksburg, MS, APR 1988.
- [7] A.L. Kuhl, J. Forbes, J. Chandler, A.K. Oppenheim, R. Spektor, and R.E. Ferguson, Confined combustion of TNT explosion products in air, 8th International Colloquium on Dust Explosions, Schaumburg, IL, USA, September 21-25, 1998.
- [8] E. Salzano, A. Basco, and F. Cammarota, Confined after-burning of display pyrotechnics and explosives, *Combustion Colloquia 2009*, 32nd Meeting on Combustion, Università Degli Studi di Napoli “Federico II”, Napoli, Italy, 26-28 April 2009.
- [9] L.D. Daily, Simulating afterburn with LLNL hydrocodes, LLNL Technical Report UCRL-TR-206313, Lawrence Livermore National Laboratory, Livermore, CA, USA, 31 August 2011.
- [10] E.L. Baker, C. Capellos and L.I. Stiel, Generalized thermodynamic equation of state for reacting aluminized explosives, *Proceedings of the 13th International Detonation Symposium*, Norfolk, VA, USA, 23-28 July 2006.

